

Hydrocarbon Index – an algorithm for hyperspectral detection of hydrocarbons

F. KÜHN*, K. OPPERMANN and B. HÖRIG

Federal Institute for Geosciences and Natural Resources (BGR),
Wilhelmstrasse 25-30, 13593 Berlin, Germany

(Received 3 September 2002; in final form 18 August 2003)

Abstract. Previous studies have shown that spectral signatures of hydrocarbon-bearing materials are characterized by prominent absorption features at 1.73 and 2.31 μm . Many other materials also show absorption features at wavelengths in the interval from 2.0 to 2.5 μm , yielding a mixed response in spectral signatures. In contrast to this wavelength range, most materials show similar spectral characteristics in the 1.73 μm range. Mainly hydrocarbon-bearing materials produce an absorption feature which is unique and prominent at 1.73 μm . A Hydrocarbon Index (HI) was developed and tested for the direct detection of hydrocarbons. The HI transforms multispectral data into a single image band that shows the distribution of hydrocarbons on the ground surface. The HI takes advantage of reflection differences around the 1.73 μm feature in hydrocarbon spectra. The HI indicates the presence of the 1.73 μm hydrocarbon absorption feature in a pixel spectrum. HI values can be easily calculated from radiance and reflectance data recorded by high signal-to-noise ratio hyperspectral scanners.

1. Introduction

Previous studies have shown that spectral signatures of hydrocarbons are characterized by absorption features at 1.73 and 2.31 μm (e.g. Clutis 1989, Kühn and Hörig 1996, Ellis *et al.* 2000, Hörig *et al.* 2001). Most researchers working in the field of hyperspectral remote sensing have used the 2.31 μm feature for the detection of hydrocarbons. The 1.73 μm feature is very close to a major water absorption maximum. Ellis *et al.* (2001) presume that this might be the reason why this feature has not been subject to investigations. Hörig *et al.* (2001) demonstrated the potential of the 1.73 μm feature for the direct detection of hydrocarbon-bearing materials. The 1.73 μm feature could be depicted clearly in radiance and reflectance spectra that were recorded for hydrocarbon-bearing materials in the field and laboratory (e.g. lubrication oil and plastics). They were also able to recognize reliably the 1.73 μm feature in HyMap pixel spectra derived from radiance and reflectance data.

The potential of the 1.73 μm hydrocarbon feature was the reason for further studies leading to the development of a Hydrocarbon Index. Plotting of the Hydrocarbon Index should highlight all pixels that cover areas containing

*Corresponding author; e-mail: friedrich.kuehn@bgr.de

hydrocarbon-bearing materials. We wanted an index that can be used similarly to the Normalized Difference Vegetation Index (NDVI). Here we report on an algorithm derived and tested for routine applications in hyperspectral remote sensing, and we demonstrate image processing examples of this index for oil and hydrocarbon detection. This Letter can be understood as a supplement to Hörig *et al.* (2001).

2. Definition of the Hydrocarbon Index

Figure 1 shows selected GER IRIS Mark V radiance field spectra that were recorded for materials at a test field on the premises of the Federal Institute for Geosciences and Natural Resources (BGR) in the Spandau district of Berlin. The test field has been described by Hörig *et al.* (2001). It consisted of specially prepared reference materials and of materials as are common for urban areas, e.g. concrete, grass and buildings. The reference areas were used to define the spectral properties of the target materials (oil-contaminated ground, etc.), to evaluate the effects of undersampling in the case of small targets, and to define the limits of the hyperspectral scanner data in the case of targets that are characterized by low-intensity spectral features. Our previous studies showed that the $1.73\ \mu\text{m}$ hydrocarbon absorption feature is unique in that portion of the spectrum, and thus can serve as a 'key feature' for detection of hydrocarbons.

Figure 2 is an enlarged plot of the $1.73\ \mu\text{m}$ hydrocarbon feature. The $1.73\ \mu\text{m}$ feature is a low energy feature but clear in that range of the spectrum. All other materials analysed showed an approximately linear to slightly curvilinear trend.

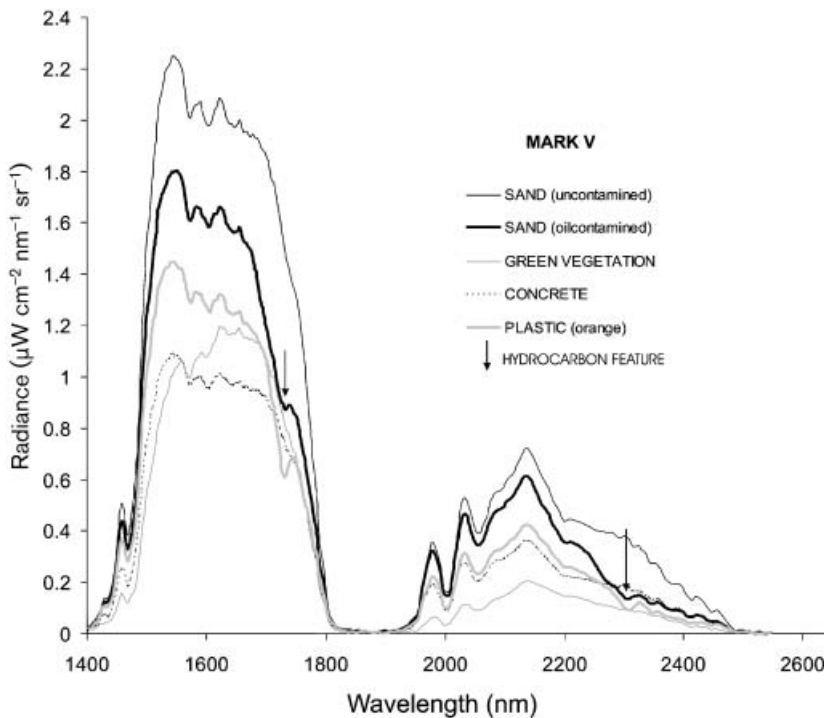


Figure 1. GER IRIS MARK V radiance spectra of oil-polluted sand and plastic showing significant $1.73\ \mu\text{m}$ absorption features.

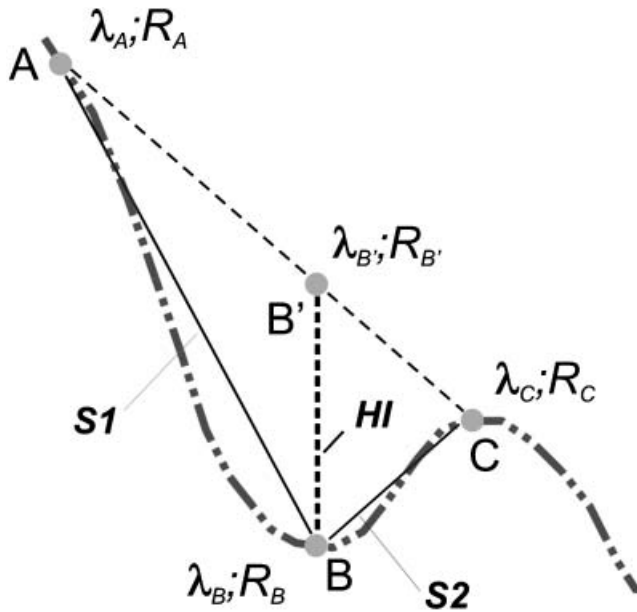


Figure 2. Enlarged $1.73 \mu\text{m}$ portion of the spectral signature (radiance) of hydrocarbon-bearing materials with 'index points' A, B, B' and C for the Hydrocarbon Index; R_i and λ_i are the radiance values and wavelengths at the 'index points'.

That uniqueness offers an opportunity to develop an algorithm for automatic selection of all pixels on hyperspectral imagery whose spectra contain the $1.73 \mu\text{m}$ hydrocarbon feature. Like the Normalized Difference Vegetation Index (NDVI), the Hydrocarbon Index (HI) should use easy-to-use mathematical algorithms, transforming multi-band data into a single band showing the presence of hydrocarbons.

Simple equations are preconditions for developing an easily used image processing tool. The equations should use only a few 'index points' for the $1.73 \mu\text{m}$ hydrocarbon feature that are reliably and unambiguously defined. Additionally, the algorithm must have the ability to depict the hydrocarbon feature even though it is a very low energy feature. To define unambiguous 'index points' that reliably describe the $1.73 \mu\text{m}$ feature we decided on the points A, B, B', and C shown in figure 2. For our HyMap data, the index points were set for the wavelengths λ_A : 1705 nm, $\lambda_B = \lambda_{B'}$: 1729 nm, and λ_C : 1741 nm.

The Hydrocarbon Index uses the vertical line $HI = BB'$ as indicator of the occurrence of oil and other hydrocarbons within the pixel. If hydrocarbon-bearing materials are present at the ground surface, the index points A, B, and C form a triangle ($HI > 0$). As an approximation, it can be assumed that the larger the HI value, the larger the hydrocarbon concentration. If no hydrocarbon-bearing material is present, the index points A, B, and C lie along a nearly straight line, and no triangle is formed ($HI = 0$). The Hydrocarbon Index can be calculated as follows:

$$HI = (\lambda_B - \lambda_A) \frac{R_C - R_A}{\lambda_C - \lambda_A} + R_A - R_B, \quad (1)$$

where $R_A; \lambda_A$, $R_B; \lambda_B$, and $R_C; \lambda_C$ are radiance/wavelength pairs for each 'index point' (cf. figure 2). For our HyMap data, the radiance values R_A , R_B , and R_C of the swirl bands 24 (1705 nm), 26 (1729 nm), and 27 (1741 nm), respectively, are inserted into

equation (1):

$$HI = \frac{2}{3}(R_{1741} - R_{1705}) + R_{1705} - R_{1729} \quad (2)$$

The HI values for equation (2) can be calculated with the ENVI Band Math Tool as follows:

$$HI = 2(float(b3 - b1))/3 + b1 - b2 \quad (3)$$

where b1 is swirl band 1705 nm, b2 is swirl band 1729 nm and b3 is swirl band 1741 nm of the HyMap radiance image.

Equations (2) and (3) can be used only for the HyMap wavelengths mentioned above. Other wavelengths may be necessary for other scanners. Equations (1–3) can also be used for reflectance data.

3. Results and discussion

3.1. HI testing

To demonstrate HI processing we applied equation (3) to a HyMap dataset recorded in 1998. The data were recorded at a flight altitude of 1137 m with 2.27 m across-track Ground-projected Instantaneous Field of View (GIFOV) and 2.84 m along-track GIFOV. More details on those data can be found in Horig *et al.* (2001). Following our concept of developing an easy-to-use method, we calculated and evaluated the HI images for HyMap radiance data. Additional HI calculations using reflectance data from the same flight did not provide more accurate results.

A HyMap colour composite image that covers part of our 1998 study area is shown in figure 3. Several reference areas are numbered: (1) sand, highly oil-contaminated (4 m × 4 m, 100 ml lubricating oil (API SF/CC type) per kg sand); (2) sand, slightly oil-contaminated (4 m × 4 m by size, 25 ml lubricating oil (API SF/CC) per kg sand), (3) plastic, (4) artificial grass and race track, (5) plastic roofs. Enlargements of reference areas 1, 2, and 3 on the BGR premises are shown in figures 3 and 4.

The colour composite image in figure 3, using near-natural colours, is based on the VIS (visible) bands 16 (Red), 10 (Green), and 3 (Blue). Figure 4 shows the Hydrocarbon Index image derived from the same data for the same area. The grey scale values were assigned using an ENVI Hue Sat Lightness 2 colour table and linear stretching of 2%. All pixels with the 1.73 μm hydrocarbon feature in their pixel spectra can be identified reliably. This can be considered as a demonstration of the suitability of the 1.73 μm Hydrocarbon Index.

3.2. Discussion

Because the 1.73 μm hydrocarbon feature is relatively low energy, optimum stretching of the grey scale may be crucial for the quality of the final HI image. The optimum stretching is most accurately determined by using reference areas containing hydrocarbon-bearing material. The most accurate HI images are obtained for urban areas and bare ground, whereas areas that are largely covered by vegetation may appear ‘noisy’ in HI imagery. Dry vegetation can further limit the use of the HI. Dark-coloured hydrocarbons are not detected reliably by the HI method.

The HI images do not allow different kinds of hydrocarbon-bearing materials to be differentiated. Combined interpretation of the results of different image

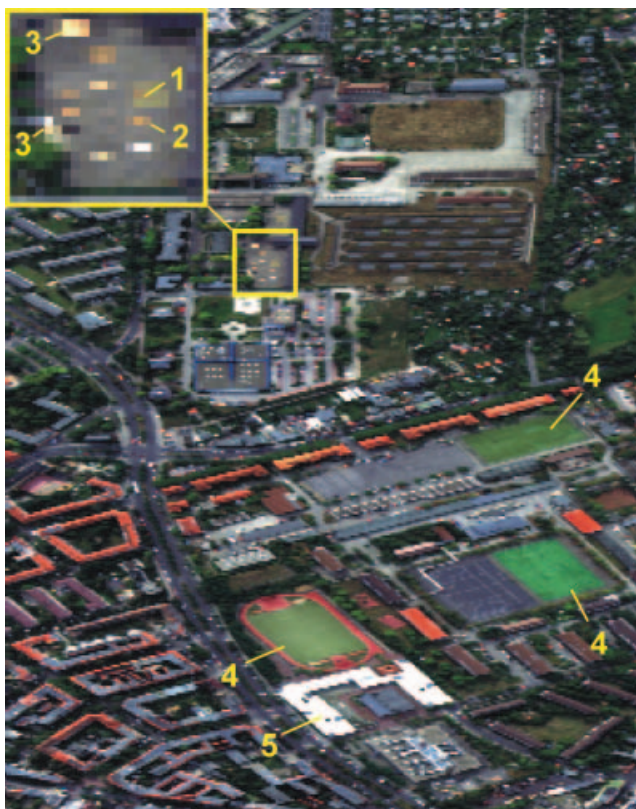


Figure 3. HyMap RGB colour composite image in near-natural colours based on VIS bands 16/R, 10/G, and 3/B; the image is of the BGR premises with (1) and (2) oil-contaminated reference areas, (3) plastic sheets, (4) artificial grass and race track, (5) plastic roofs; insert above left: zoomed section.

processing methods which include different portions of the spectrum was optimal for differentiation. To distinguish oil-contaminated ground from other materials made of hydrocarbons, colour composite images based on HyMap bands in the visible and the near-infrared portions of the spectra can be used. In these parts of the spectrum, the colours of the objects help distinguish, for example, between plastics, artificial grass, roofing felt, and oil-contaminated ground (figure 3). Detection and distinction of hydrocarbons can further be aided by RGB colour composite images that are based on bands using the $1.73\ \mu\text{m}$ hydrocarbon absorption feature (cf. Hörig *et al.* 2001), and by images that were calculated using standard spectral mapping methods.

We consider that the fact that the HI method can be applied to radiance data is of significance for the efficiency of the method for hydrocarbon detection. Precondition is a precise calibration of the sensor, which should have a high signal-to-noise ratio. In this case, costly atmospheric correction is not necessary. Limited correction of the data is a precondition for the rapid application of the method for hydrocarbon detection in the case of an accident with oil. However, the HI values can be calculated for atmospherically corrected reflectance data, too.

We have tested the HI algorithm using HyMap radiance and reflectance data of differing quality. Our experience shows that HI processing provides reliable results

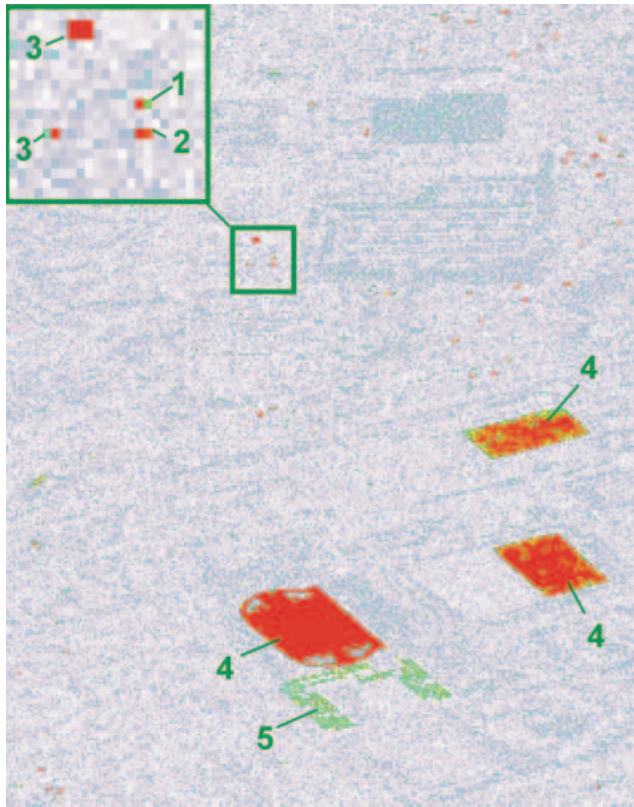


Figure 4. HyMap Hydrocarbon Index image (HI image) derived from the same dataset used for figure 3 using equation (3); red pixels indicate the presence of hydrocarbon-bearing materials; the grey scale values were assigned using ENVI Hue Sat Lightness 2 colour table.

if the hyperspectral data are of high radiometric quality, recorded with precisely calibrated scanners and little affected by atmospheric particles that cannot be removed by standard atmospheric corrections. Further factors that may negatively affect the quality and the reliability of HI processing are high flight altitudes, and large pixel sizes. In some cases, dark and very light-coloured objects and shadowed objects were incorrectly classified. Independent of the quality of the data, field checks should be the final task of HI-based hydrocarbon detection using hyperspectral remote sensing.

4. Summary

A Hydrocarbon Index (HI) was derived and tested. This study showed that a Hydrocarbon Index applied to airborne hyperspectral remote-sensing data can be used to efficiently detect hydrocarbons. The HI was derived for the hydrocarbon absorption feature at $1.73 \mu\text{m}$. High-performance hyperspectral imaging systems make it possible to process HI images even if this feature appears only weakly in the pixel spectra. Hydrocarbon-bearing materials, and oil-contaminated ground in particular, could be detected and located using HI images.

Using a precisely calibrated hyperspectral sensor with a high signal-to-noise ratio, radiance data can be used for HI processing. It was not necessary to apply

atmospheric corrections. This study demonstrated that the Hydrocarbon Index has the potential to become a useful image processing algorithm for the hyperspectral detection of hydrocarbons.

Acknowledgments

The authors thank the Environmental Baseline and GIS & Remote Sensing teams of ChevronTexaco in Richmond and San Ramon, California, for discussions that led to this study on the use of the 1.73 μm hydrocarbon feature to derive a Hydrocarbon Index. We further thank F. Lehmann, F. Oschütz and T. Bucher (German Aerospace Centre, DLR, Berlin-Adlershof) for discussions and advice on calibration and correction of HyMap data. R.C. Newcomb is thanked for improvement of the English text.

References

- CLUTIS, E. A., 1989, Spectral reflectance properties of hydrocarbons: remote sensing implications. *Science*, **245**, 165–168.
- ELLIS, J. M., DAVIS, H. H., and QUINN, M. B., 2000, Airborne hyperspectral imagery for the petroleum industry. *Proceedings of the 14th International Conference on Applied Geologic Remote Sensing, Las Vegas, Nevada, 6–8 November 2000*, pp. 89–96.
- ELLIS, J. M., DAVIS, H. H., and ZAMUDIO, J. A., 2001, Exploring for onshore oil seeps with hyperspectral imaging. *Oil and Gas Journal*, **99**, 49–58.
- HÖRIG, B., KÜHN, F., OSCHÜTZ, F., and LEHMANN, F., 2001, Hyperspectral remote sensing to detect hydrocarbons. *International Journal of Remote Sensing*, **22**, 1413–1422.
- KÜHN, F., and HÖRIG, B., 1996, Environmental remote sensing for military exercise places. *Remote Sensing and GIS for Site Characterizations: Applications and Standards, ASTM STP 1279, American Society for Testing and Materials*, 5–16.